J. Membrane Biol. 76, 235–251 (1983)

The Journal of
Membrane Biology

Competitive Blocking of Epithelial Sodium Channels by Organic Cations: The Relationship between Macroscopic and Microscopic Inhibition Constants

Jack H.-Y. Li and Bernd Lindemann

2nd Department of Physiology, Universität des Saarlandes, 6650 Homburg/Saar, Federal Republic of Germany

Summary. Fluctuation analysis of Na current passing the apical membrane in the skin of *Rana ridibunda* was used to study the kinetics of Na-channel blocking by several organic cations present in the outer solution together with 60 mM Na. The ratios of the apparent off-rate and on-rate constants (the microscopic inhibition constants) thus obtained for triamterene, triaminopyrimidine (TAP), 5,6-diCl-amiloride, 5H-amiloride and amiloride itself are found to be in the mean about sevenfold smaller than the corresponding inhibition constants obtained from macroscopic dose-response curves. The apparent discrepancy is explicable by competition of the organic blocker with the channel block by Na ions (the self-inhibition effect). The type of interaction between extrinsic blockage and self-inhibition may be purely competitive or mixed. However, in case of mixed inhibition the competitive component must dominate the noncompetitive component by at least seven to one.

Key Words epithelial transport · apical Na permeability of frog skin · fluctuation analysis · extrinsic blockers · amiloride analogs · triamterene · triaminopyrimidine · dose-response curves · competition kinetics

Introduction

In the past, amiloride has been used rather extensively as an extrinsic blocker of apical Na channels of amphibian epithelia. By current fluctuation analysis of extrinsic blockage the blocking rate constants, channel currents and channel densities were estimated (e.g. Lindemann & Van Driessche, 1976; Van Driessche & Lindemann, 1979; Li, Palmer, Edelman & Lindemann, 1982; Palmer, Li, Lindemann & Edelman, 1982). In the course of this work we noticed that the macroscopic inhibition constant of amiloride is significantly larger than the ratio of blocking rate constants (i.e. the microscopic inhibition constant; *see* Fig. 6C in Li et al., 1982). In the present paper this observation is extended to four other organic cations, which block the Na channels reversibly much in the fashion of amiloride, but with different rate constants. In all cases we find the macroscopic inhibition constant to be larger than the microscopic inhibition constant. The phenomenon is explicable by competition between the organic blocker and the Na self-inhibition mechanism.

Our results have been presented at the 1981 fall meeting of the Deutsche Physiologische Gesellschaft (Li & Lindemann, 1981*a*).

List of Symbols

Na_o	Na ion activity in apical (mucosal) solution [mM]
A_o	amiloride concentration in apical solution [μM]
AA_o	concentration of an amiloride analog [μM or mM]
TAP	triaminopyrimidine
T	triamterene
BIG	benzimidazolyl-guanidine
PCMPS	parachloromercuri-phenylsulfonate
I_{Na}	amiloride-blockable component of the macroscopic current passing the apical membrane [μamp cm^{-2}]
a	membrane area [cm^2]
P_{Na}	permeability of the apical ensemble of amiloride-blockable Na channels [cm sec^{-1}]
F	Faraday's constant [coul mol^{-1}]
K_N	inhibition constant [mM] of Na self-inhibition obtained macroscopically but in the absence of added organic blockers
K_{AA}^{ma}	macroscopic inhibition constant (or Michaelis Menten constant) [μM or mM] of the extrinsic blocker AA (amiloride analog) as obtained from the inflection point of a dose-response curve
K_{AA}^{mi}	microscopic inhibition constant [μM or mM] of blocker AA as obtained from noise analysis as the negative intercept of a *linear* rate-concentration plot with the abscissa ($=k_{off}/k_{on}$)
K_{AA}	ratio of the true rate constants (e.g. $K_A = k_{20}/k_{02}$, $K_N = k_{10}/k_{01}$)
K'_{AA}	ratio of blocking rate constants of AA at a

channel already closed by the self-inhibition, in the case of mixed inhibition

k_{off}, k_{on} apparent off-rate constant [sec^{-1}] and on-rate constant [$sec^{-1}\ \mu M^{-1}$] at room temperature as obtained by noise analysis from a linear rate-concentration plot. The values of these rate constants may include competitive effects and partition coefficients

$k_{10}, k_{01}, k_{20}, k_{02}$ true off-rate and on-rate constants as expected in the absence of competition of blockers. These constants still include concentration effects due to partitioning but no competitive effects. The subscripts refer to transition between state 0 (conducting), state 1 (closed by the Na self-inhibition) and state 2 (blocked by an extrinsic blocker) of the Na channel

α $k_{off}/k_{20} = K_{AA}^{mi}/K_{AA}$

f_c^{AA} corner frequency [Hertz] of a Lorentzian current power density spectrum induced by blocker AA. A is used for amiloride, N for the Na self-inhibition.

τ $=[2\pi f_c]^{-1}$, relaxation time constant [sec] = inverse characteristic rate of blockage close to equilibrium

λ_h, λ_l characteristic rates of blockage [sec^{-1}], high (h) and low (l), due to two competing blockers

S_o plateau-power of blocker-induced Lorentzian current power density spectra (one-sided) [amp^2 sec]

i Na current [amp] passing a single channel when not blocked (state 0)

N_0, N_1, N_2, N_{12} area density [cm^{-2}] of Na channels in state 0 (conducting), state 1 (blocked by Na) and state 2 (blocked by amiloride or one of its analog). In state 12 (mixed inhibition) the channel is blocked at the same time by Na and amiloride (or one of its analogs). This state is excluded in pure competitive inhibition. The total density of electrically detectable channels is $N = N_0 + N_1 + N_2 + N_2$

SD standard deviation

Materials and Methods

Rana ridibunda of East European origin were bought from Firma Stein, Lauingen-Donau, Germany. They were kept in tanks at 10° to 15° C, unfed but having free access to running tap water. A few days before the experiment the frogs were placed into tanks at room temperature (18° to 22° C) and bathed in clean deionized water. Toads (*Bufo marinus*, Mexican origin) were obtained from Lemberger Assoc. (Wisconsin) and kept unfed at room temperature. After double-pithing, the abdominal skin of *R. ridibunda* or the urinary bladder of *B. marinus* was quickly cut out and mounted with the serosa backed by a filter paper on a ring of 3 cm^2 free cross-sectional area. This ring was then inserted between two Lucite® half-chambers. A hydrostatic pressure of 10 cm water column was applied continuously to hold the preparation against the filter paper, thus reducing microphonics in the noise records. Between the Lucite and the apical side of the epithelium an undercured silicon washer was inserted to achieve good sealing with minimal mechanical force and to minimize edge damage.

When information on the noise components at higher frequencies was required, a ring of only 0.12 cm^2 free cross-sectional area was used. In this case partial covering of the center area with the sealing material was difficult to avoid and reduced the effective exposed tissue area further. With a smaller area and, thereby, a higher absolute impedance value, the background noise introduced by the voltage clamp at higher frequencies was reduced and the high frequency limit could be moved from 110 to 400 Hz by changing filters and sample rate.

If not otherwise stated, skins or urinary bladders were depolarized with a K_2SO_4 or KCl-sucrose serosal solution, respectively, for more than 1 hr before measurements. These serosal K-Ringer's were of the same composition as those used by Fuchs, Hviid Larsen and Lindemann (1977) and Palmer, Edelman and Lindemann (1980). Unless stated otherwise, the apical solution during noise measurements was a Na_2SO_4 solution of 60 mM Na activity buffered with 3.5 mM K-phosphate at pH 5.5. This pH has the advantage of increasing the concentration of protonated blocker molecules (*see* Table for pK_a values). All solutions were used at room temperature. During noise recordings aeration of the serosal solution was stoped and perfusion of the mucosal chamber was lowered to about 1 ml/min.

For the recording of Na current fluctuations induced by the organic cations, the chamber was placed inside a grounded metal box shock-mounted on 4 springs. This box and the voltage clamp were enclosed by a larger Faraday's cage. The low-noise transistor-input clamp described by Van Driessche and Lindemann (1978) was used with a high-pass RC filter set at 0.07 Hz and an anti-aliasing filter set at 140 Hz. The clamp voltage was set to 0. When the small area preparation was used, the anti-aliasing filter was set to 500 Hz, the high-pass filter to 0.25 Hz and the sample rate to 1,638 Hz. Both the short-circuit current and the filtered noise signal were monitored continuously on a strip chart recorder and an oscilloscope, respectively. The latter signal was digitized by the 10 bit A/D converter of the minicomputer (NOVA 1230, Data General) at intervals of 2.44 or 0.61 msec for a period of 10 or 2.5 sec, depending on the frequency range being investigated. The resulting time series of 4096 data points were Fourier-transformed, and the current power density was computed on line and monitored on an XY-display. Twenty or more spectra were generally recorded, averaged and condensed by averaging along the frequency axis as described before (Li et al., 1982). The mean spectral data were then stored on disk for further evaluation.

Current power density spectra taken at several blocker concentrations were fitted with a computer program which permitted the subtraction of the commonly observed low frequency spectral component (e.g. Lindemann & Van Driessche, 1978) from the Lorentzian component. However, this subtraction was seldom necessary. In most cases it was sufficient to enter the frequency limits for fitting of the Lorentzian component. Plateau power (S_o) and corner frequency (f_c^A, frequency at half plateau power) were then obtained as fitting parameters of a least-squares procedure.

The higher relaxation rate $1/\tau_2$ of extrinsic blockage was obtained from the corner frequency of the Lorentzian multiplied by 2π, and analyzed with

$$1/\tau_2 = 2\pi \cdot f_c^A = k_{on} \cdot A_o + k_{off} \quad (1)$$

where A_o is the amiloride concentration in the outer solution, and k_{on} and k_{off} are the apparent rate constant for pseudo-first-order kinetics. Corresponding equations were

used for the other extrinsic blockers. The plots of $2\pi f_c$ versus blocker concentration (rate concentration plots) were linear (Figs. 2*B*, 3*B*, 4*A*, 4*D*, 6*C*, 7*B*, 8*C*), supporting the assumption of pseudo-first-order kinetics.

The apparent rate constants of extrinsic blockage were obtained from the rate concentration plots: k_{on} as the slope, k_{off} as the ordinate intercept. They are only 'apparent' rate constants because k_{on} includes partition coefficients of the charged blocker between bulk solution and the vicinity of the receptor at the Na channel, as well as possible effects of competing higher rate blockers, which decrease the apparent value. k_{off} includes competition effects of a lower rate blocker, which increase the apparent value as discussed below (Eq. 8).

Unless stated otherwise, values reported are the means ±standard deviation.

Theory

The analysis of blocker-induced Lorentzians is based on a three-state model for apical Na channels, where the extrinsic blocker and the Na self-inhibition compete for conducting channels. Evidence for the existence of this competition phenomenon arises mainly from published work on macroscopic dose-response curves and from the published evaluations of Lorentzian plateaus as summarized in the Discussion. Further evidence is provided by our present results. Below we shall review the equations needed in this study, emphasizing the assumptions used in the derivation and their justification.

The competition phenomenon may be formulated in terms of channel densities. With the index 0 designating conducting channels, 1 channels blocked by self-inhibition and 2 channels blocked by amiloride, we obtain the overall reaction scheme

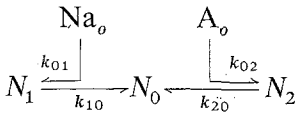

for pure rather than mixed competitive inhibition. The rate constants are indicated in this scheme. The dissociation constants are

$$K_N = k_{10}/k_{01}, \quad K_A = k_{20}/k_{02}. \tag{2}$$

The sum

$$N = N_0 + N_1 + N_2 \tag{3}$$

will be called the density of electrically detectable channels. The steady-state probabilities to find a channel in one of the three states are

$$P_0 = (1 + \mathrm{Na}_o/K_N + \mathrm{A}_o/K_A)^{-1}$$

$$P_1 = (\mathrm{Na}_o/K_N) \cdot P_0$$

$$P_2 = (\mathrm{A}_o/K_A) \cdot P_o = (1 + K_A/A_o)^{-1}. \tag{4}$$

From them the Michaelis Menten constant of macroscopic dose-response curves is obtained as

$$K_A^{ma} = K_A(1 + \mathrm{Na}_o/K_N). \tag{5}$$

It will be called the macroscopic inhibition constant, in contradistinction to the microscopic inhibition constant

$$K_A^{mi} = k_{off}/k_{on} \tag{6}$$

which is obtained from induced Lorentzians by means of linear rate concentration plots.

Rate Analysis

The kinetics of two competing reactions are characterized by the two relaxation time constants τ_1 and τ_2. Their values can be obtained from the change of N_0 with time in response to a small perturbation in Na_o or A_o. Alternatively, τ_1 and τ_2 can be retrieved from the spontaneous fluctuations of N_0. The noise generated by two competing blockers results in power density spectra with two additive Lorentzian components (Lindemann & Van Driessche, 1978). Their corner frequencies are related to the inverse time constants by

$$1/\tau_1 = 2\pi \cdot f_c^N = \lambda_l$$

$$1/\tau_2 = 2\pi \cdot f_c^A = \lambda_h. \tag{7}$$

These are the 'chemical relaxation rates' or 'characteristic rates' near equilibrium.

Rate analysis is based on the dependence of the chemical rates on the blocker concentrations. The corresponding theoretical relationships are obtained from the kinetic differential equations by standard algebraic techniques (e.g., Hammes, 1968). In full generality the solutions are complicated and will not be reproduced here. A simplification is obtained if $(1/\tau_1) \ll (1/\tau_2)$. Then the higher characteristic blocking rate is given by

$$1/\tau_2 = k_{02}\,\mathrm{A}_o + k_{02}\,\beta N_0 + k_{20} \tag{1a}$$

where β is a constant which converts the channel density N_0 (cm^{-2}) into the units of A_o. Equation (1a), in which N_0 is a function of A_o and Na_o (*see* Eq. 4), represents second-order kinetics near equilibrium. In this case plots of $1/\tau_2$ versus A_o are nonlinear. However, when

$\beta \cdot N_0$ is negligible with respect to A_o, we obtain

$$1/\tau_2 = k_{02} A_o + k_{20} \quad (1b)$$

i.e. pseudo-first-order kinetics and corresponding linear rate concentration plots. The fact that linear plots are obtained with amiloride justifies the pseudo-first-order approach (Eq. 1).

If the two relaxation chemical rates are far apart but not extremely so, one obtains for negligible $\beta \cdot N_0$

$$1/\tau_2 = k_{02} A_o + k_{20} + k_{01} Na_0. \quad (1c)$$

In this case the rate concentration plot is still linear. Its ordinate intercept is given by

$$k_{off} = k_{20} + k_{01} Na_o \quad (8)$$

and the slope by $k_{on} = k_{02}$. Therefore

$$K_A^{mi} = K_A \left(1 + \frac{k_{10}}{k_{20}} \frac{Na_o}{K_N}\right) = K_A \frac{k_{off}}{k_{20}}. \quad (6a)$$

Plateau Analysis

Of the two Lorentzians expected from the competitive blocking, the one of higher relaxation rate is found in the 1 to 50 Hz band which is a convenient frequency range for steady-state noise recording. We analyze the plateaus of these induced Lorentzians with the assumptions that amiloride blocks the Na channels in a one-to-one and all-or-none manner. These assumptions seem reasonable since macroscopically amiloride blocks cellular Na uptake almost completely (e.g. Rick, Dörge & Nagel, 1975) and in the epithelia used the Hill coefficient is near unity (e.g. Li et al., 1982). The one-to-one assumption is implicit in the kinetic scheme (Eq. 4) and the all-or-none assumption is needed for the use of Eq. (10) (*see below*).

For simple open/close kinetics without competition (K_N very large) the power of the amiloride-induced plateau of one-sided spectra is given by

$$S_o = 4aNi^2 P_0 P_2 \tau_2 \quad (9)$$

where i is the current passing a channel when open, and a the membrane area. With

$$I_{Na} = iNP_0 = iN_0 \quad (10)$$

in which I_{Na} is the macroscopic amiloride blockable Na current/cm^2, one obtains

$$\frac{S_o}{I_{Na}} = 4aiP_2\tau_2 = \frac{4ai}{2\pi f_c^A \cdot (1 + K_A/A_o)}. \quad (11)$$

Since without competition K_A is obtained as K_A^{mi} from f_c^A (rate concentration plot), i can be computed from

$$i = (1.57 \cdot S_o \cdot f_c^A) \cdot (1 + K_A/A_o) \cdot (a \cdot I_{Na})^{-1} \quad (11a)$$

where $1.57 \cdot S_o \cdot f_c^A$ is the variance of I_{Na}.

With competition (K_N small) one obtains the different expression

$$\frac{S_o}{I_{Na}} = 4ai \cdot \tau_2 \cdot \frac{P_2}{P_0 + P_2}. \quad (12)$$

It may be noted, however, that

$$\frac{P_2}{P_0 + P_2} = \frac{1}{1 + K_A/A_o} \quad (13)$$

which makes Eq. (12) identical with Eq. (11). The difference is merely, that in case of competition a K_A^{mi} value larger than K_A may be obtained from the rate concentration plot (*see* Eq. 6a). For $K_A^{mi} = K_A$ we may state that the estimation of i from the Lorentzian plateau of the higher rate blocker will yield the same value with competition kinetics used or neglected. The error which results when a K_A^{mi} value larger than K_A is used instead of K_A, can be evaluated by rewriting Eq. (11a) as

$$i = (1.57 \cdot S_o \cdot f_c^A) \cdot (1 + K_A^{mi}/\alpha \cdot A_o) \cdot (a \cdot I_{Na})^{-1} \quad (11b)$$

where $\alpha = K_A^{mi}/K_A = k_{off}/k_{20}$. The observed value of f_c^A need not be corrected with α since it already contains the effect of competition. For amiloride the exact value of α is not known, but is expected to range between one and two. It can be seen that for large A_o values, typically 7- to 45-fold larger than K_A^{mi}, the influence of α tends to vanish.

N_0 is obtained as the current ratio

$$N_0 = I_{Na}/i \quad (10a)$$

provided the microscopic blocking event is 'all-or-none.' Furthermore, since $P_0 + P_2 = P_0 \cdot (1 + A_o/K_A)$, the density of directly 'amiloride accessible' channels

$$N_0 + N_2 = (I_{Na}/i)(1 + A_o/K_A) \quad (14)$$

can be calculated. The following, final step of the analysis requires competition theory. In case of competition the channel density N_1 is given by

$$N_1 = N \cdot (Na_o/K_N)/(1 + Na_o/K_N + A_o/K_A) \quad (15)$$

and should vanish at saturating A_o. Then N can be estimated as $N_0 + N_2$ by extrapolating

this quantity (Eq. 14) to infinite A_o (Li et al., 1982). Thus values for N_0, N_1 and N_2 are obtained by analyzing the Lorentzian plateaus.

Results

Amiloride

The blocking properties of amiloride were reinvestigated for mucosal pH values of 5.5 since amiloride served as a reference for other blockers used at this pH in the experiments detailed below. The macroscopic inhibition constant of amiloride, K_A^{ma}, was obtained for the concentration range useful in noise analysis in the following way. In the presence of 60 mM mucosal Na-activity (Na_o), a set of amiloride concentrations (A_o) between 0 and 10 μM was sequentially employed to reduce the short-circuit current of K-depolarized skins. From the steady-state currents thus obtained, the Na-current I_{Na} was computed by subtraction of the current component insensitive to 80 μM amiloride. Following the reasoning of Fuchs et al. (1977), Na_o/I_{Na} was then taken as an estimate of $(F \cdot P_{Na})^{-1}$ and plotted against A_o (Fig. 1*A*). A straight line was fitted to the data points and its intercept with the abscissa taken to indicate the macroscopic inhibition constant, K_A^{mA}. Values ranging between 1 and 3 μM were found in the presence of 60 mM Na_o at pH 5.5. Figure 1*B* shows mean data of this kind in the more conventional semilogarithmic dose-response plot. Note that only A_o values in the range of K^{ma} or larger than K^{ma} were used since only these yield evaluable Lorentzians if the off-rate constant is low, as in the case of amiloride.

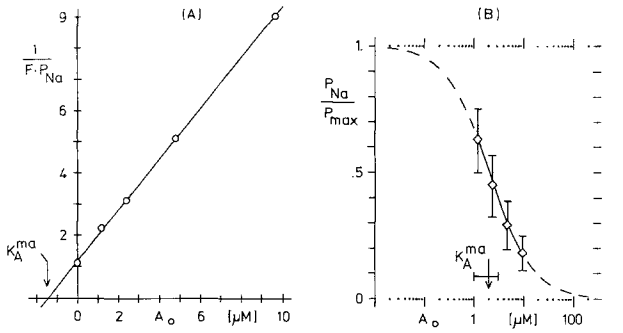

Fig. 1. Macroscopic data obtained in the presence of amiloride. K-depolarized short-circuited frog skin, $Na_o = 60$ mM, mucosal pH 5.5. *A*: Plot of reciprocal steady-state P_{Na} versus apical amiloride concentration A_o. One experiment. The macroscopic inhibition constant K_A^{ma} is obtained as the intercept of the regression line with the abscissa. *B*: Normalized dose-response curve. Mean of 58 experiments like that of panel *A*. The vertical bars represent ±1 SD. The mean K_A^{ma} was determined to 1.79 ±0.97 μM.

Amiloride-induced spectral components of current power densities obtained in the presence of 60 mM Na_o with a clamp voltage of zero are shown in Fig. 2*A* for four amiloride concentrations. For the concentration range indicated each Lorentzian plateau extends over or beyond one frequency decade. Its power decreases with increasing A_o. Except for high A_o, the rolloff at high frequencies could also be observed over at least one decade. It has a slope of −2. The spectra were fitted with Lorentzian functions extending over the frequency range indicated by the solid lines. At low frequencies the noise power often exceeded the plateau values. However, except for a few cases it was not necessary to include this noise component in the fit (*see* Materials and Methods). The corner frequencies increased with increasing A_o (arrows). Multiplication with 2π yields the higher characteristic rate of blockage (Eq. 1), which was plotted against A_0 (Fig. 2*B*). As before at pH 7.2 (e.g. Lindemann & Van Driessche, 1977), a linear rate-concentration relationship was obtained for pH 5.5. The regression line, based on data from 58 skins of *R. ridibunda*, yields an apparent on-rate constant, $k_{on} = 13.17 \pm 1.88\,\text{sec}^{-1}\,\mu\text{M}^{-1}$ (slope), an off-rate constant, $k_{off} = 3.93 \pm 1.47\,\text{sec}^{-1}$ (ordinate intercept), and a microscopic inhibition constant of $K_A^{mi} = 0.30 \pm 0.13$ μM (negative intercept with abscissa). Note that K_A^{mi} is about one-sixth of K_A^{ma} (mean values).

The change of plateau power per ampere of macroscopic Na current with A_o is shown in Fig. 2*C* for one experiment. The solid line is a fit with the theoretical relationship

$$\frac{S_o}{I_{Na}} = 4ai\tau_2 \frac{A_o/K_A}{1 + A_o/K_A} = \frac{4ai}{k_{20}} \cdot \frac{A_o/K_A}{(1 + A_o/K_A)^2} \quad (12a)$$

which is valid for competition between A_o and Na_o, provided amiloride is the higher rate blocker and the two chemical rates are sufficiently different, such that $K_A^{mi} \approx K_A$ (*see* Theory).

The arrows indicate K_A^{mi} as derived from the maximum of the theoretical curve, and the value of K_A^{ma} obtained in this experiment from macroscopic data.

5,6-diCl-Amiloride

This analog differs from amiloride in that in addition to the chlorine at position 6 a second chlorine is bound at position 5 of the pyrazine

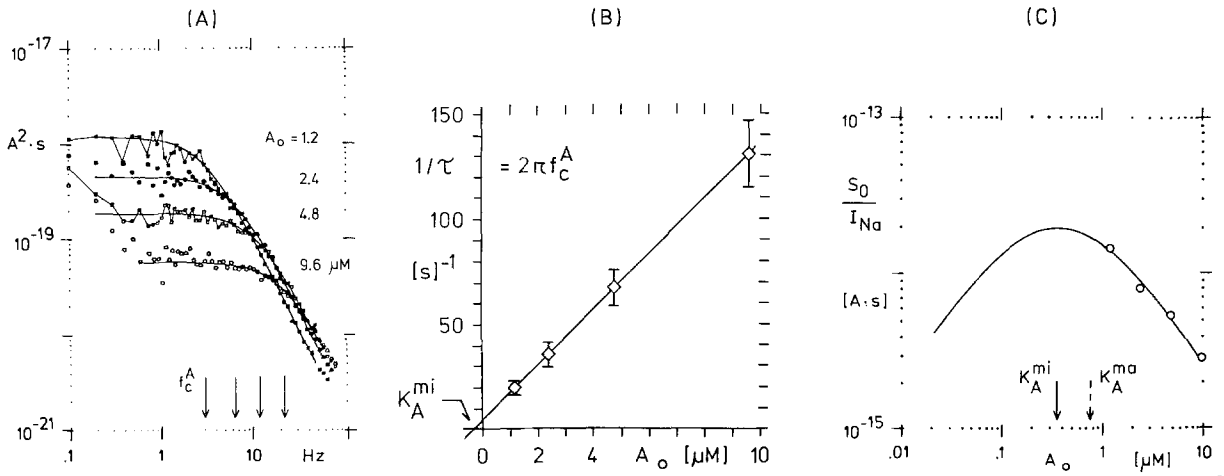

Fig. 2. Microscopic data obtained in the presence of amiloride. K-depolarized, short-circuited frog skin of 3 cm^2, Na_o = 60 mM, mucosal pH 5.5. *A*: Current power density spectra (referred to 3 cm^2 of chamber area) taken at the amiloride concentrations indicated. The smooth lines are fitted Lorentzians drawn only over the data range used for fitting. *B*: Rate concentration plot $1/\tau = 2\pi f_c^A = k_{on} A_o + k_{off}$ is plotted versus A_o. The mean f_c^A's, from Lorentzians like those of panel *A*, were used ($n = 58$; ± SD). The microscopic inhibition constant $K_A^{mi} = k_{off}/k_{on} = 0.3$ μM is sixfold smaller than the mean K_A^{ma} of 1.79 μM (Fig. 1). *C*: Least-squares fit of (S_o/I_{Na}) as a function of A_o. Data from the experiment of panel *A*, but S_o referred to 1 cm^2 area. The maximum is located at $A_o = K_A^{mi} < K_A^{ma}$ (*see* Eq. 12a). K_A^{ma} was unusually small in this experiment

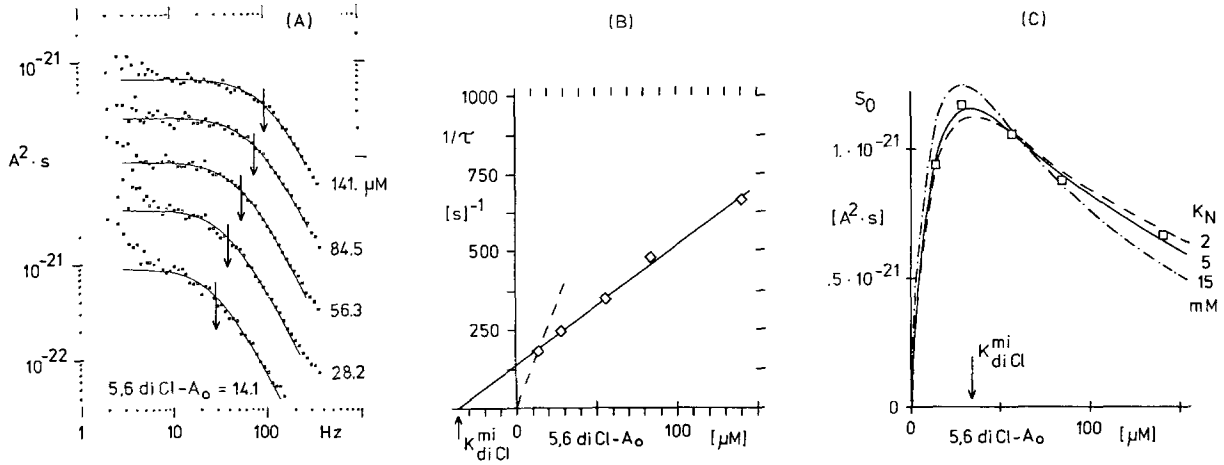

Fig. 3. Microscopic data obtained in the presence of 5,6-diCl-amiloride, analog L592,272-01U01. K-depolarized short-circuited frog skin, Na_o = 60 mM, mucosal pH 5.5. An exposed membrane area of about 0.1 cm^2 was used, the anti-aliasing filter set to 500 Hz and the sample frequency increased to 1638 Hz. *A*: Current power density spectra at blocker concentrations of 5,6-diCl-A_o = 14.1, 28.2, 56.3, 84.5 and 140.8 μM. Since the plateaus are all close to 10^{-21} A^2 sec (*see* panel *C*), each spectrum was shifted upward with respect to its lower neighbor by a factor of 3. The ordinate scale was drawn only for the uppermost and the lowest spectrum. *B*: Rate-concentration plot. For comparison the amiloride rate concentration plot is indicated by a dashed line (from Fig. 2*B*). 5,6-diCl-amiloride as a smaller on-rate (slope) and a larger off-rate constant (ordinate intercept) than amiloride. The value of K_{diCl}^{mi} is 37.4 μM. *C*: Plateau power-concentration plot. Note that, similar to the triamterene spectra (Fig. 6*B*), the plateau of the Lorentzian increases with the blocker concentration as long as the latter is smaller than 0.5 K^{mi}. The drawn-out curve is a least-squares fit with Eq. (12b), in which the following values were used: $aN = 2.29 \times 10^8$, $i = 0.10$ pA, $K_N = 5$ mM, $k_{20} \approx k_{off} = 141.74$ sec^{-1} and $K_{diCl} \approx K_{diCl}^{mi} = 37.4$ μM

ring, replacing the NH_2 group. The macroscopic dose-response curve, obtained like that for amiloride at 60 mM Na_o and pH 5.5, yielded a high K_{diCl}^{ma} of 270 μM. The power density spectrum contains blocker-induced Lorentzians (shown for 5 analog concentrations of a small area experiment in Fig. 3*A*). The rate-concentration plot of this experiment (Fig. 3*B*) yielded a straight-line relationship with $k_{on} = 3.8$ sec^{-1} μM^{-1} (not corrected for incomplete protonation at pH 5.5), $k_{off} = 141.74$ sec^{-1} and $K_{diCl}^{mi} = 37.4$ μM. The means of 6 small area experiments are given in the Table. Note that again K^{ma} is clearly larger than K^{mi}.

Table. Rate constants and inhibition constants of amiloride, triamterene, TAP and two structural analogs of amiloride[a]

Tissue	Drug	pK_a[b]	pH	k_{on} ($sec^{-1}\,\mu M^{-1}$)	k_{on}[c] org. cation ($sec^{-1}\,\mu M^{-1}$)	k_{off} (sec^{-1})	K^{mi} (μM)	n	K^{ma} (μM)	n
FS[d]	amiloride	8.7	5.5	13.17±1.88[f]	13.18±1.88	3.93±1.47	0.30±0.13	58	1.79±0.97	58
FS			7.5	12.25±0.66	13.02±0.70	4.41±0.96	0.36±0.09	4	4.28±2.48	4
TB[e]			7.5	16.86±1.86	17.92±1.98	2.66±2.40	0.17±0.17	9	0.43±0.33	10
FS	triamterene	6.2	5.5	13.35±1.48	16.02±1.78	36.20±6.73	2.78±0.78	6	18.15±13.95	12
FS			7.0	5.06±0.91	36.99±6.65	34.02±2.25	6.94±1.52	6	54.44±13.43	6
TB			7.0	8.81±1.20	64.40±8.77	25.29±1.86	3.03±1.86	5	7.90±2.74	5
FS	5H-amiloride	7.0	5.5	3.32±1.24	3.43±1.28	10.89±3.82	4.02±2.64	9	32.9 ±10.7	9
FS	5,6-diCl-amiloride	6.6	5.5	5.16±1.03	5.57±1.11	151 ±36.9	29.6 ±2.8	6	216 ±112	4
FS	TAP	6.7	5.5	-	-	-	330 ±80	4	4,150 ±133	11

[a] The K^{mi} of all these reversible Na channel blockers is found to be smaller than the respective K^{ma}.
[b] Values from the literature.
[c] Values of pK_a listed in column 3 were used in the calculation; a correction of the on-rate for incomplete protonation is not necessary if the compared values of K^{mi} and K^{ma} were obtained at the same pH. Values shown for K^{mi} and K^{ma} are also uncorrected.
[d] FS = abdominal skin of *R. ridibunda*.
[e] TB = urinary bladder of *B. marinus*. Data are from Li et al. (1982).
[f] Means ±SD.

The power densities of the Lorentzian plateaus increased with analog concentration at low concentrations, but decreased at higher concentrations (Fig. 3 *C*). In principle this behavior is always expected (compare theoretical curve of Fig. 2 *C*) because the product of probabilities for a channel to be open and blocked, which is contained in the expression for the Lorentzian plateau (Eq. 9), passes through a maximum when the blocker concentration is increased. However, Lorentzians corresponding to the low concentration part of the convex curve will be observed only when the corner frequency of the extrinsic blocking process is sufficiently high. The 5,6-diCl-amiloride, by virtue of its high off-rate, provides an example. The solid line of Fig. 3 *C* was obtained by a least-squares fit of

$$S_o = \frac{4aNi^2}{k_{20}} \frac{A_o/K_A}{(1+Na_o/K_N+A_o/K_A)(1+A_o/K_A)^2} \quad (12b)$$

to the data points. The equation is obtained from Eq. (12a) by combination with

$$I_{Na} = iN_0 = iN \cdot (1+Na_o/K_N+A_o/K_A)^{-1}. \quad (10b)$$

The maximum of S_o is expected between $0.5 \cdot K_A$ and K_A, depending on the numerical value of Na_o/K_N. In the fit we used $K_A = K_A^{mi}$ and $k_{20} = k_{off}$. K_N was the adjustable parameter. It appears that with $K_N = 5$ mM the theoretical equation for competitive blocking by 5,6-diCl-amiloride and Na ions fits the data reasonably well.

5H-Amiloride

In this analog the $-NH_2$ group at position 5 of the pyrazine ring is replaced by hydrogen. K_{5H}^{ma} was estimated in nine experiments in the presence of 60 mM Na_o (pH 5.5), yielding a mean value of 32.9±10.7 μM. The concentrations needed to obtain 5H-amiloride induced Lorentzians in the presence of 60 mM Na_o (pH 5.5) were about 5 times larger than those of amiloride. The corner frequencies were also larger and the rate-concentration plot (Fig. 4 *A*) showed this to be due to a high off-rate. The apparent rate constants, determined from this plot, are $k_{on} = 3.32 \pm 1.24\ sec^{-1}\,\mu M^{-1}$ (not corrected for incomplete protonation at pH 5.5) and $k_{off} = 10.89 \pm 3.82\ sec^{-1}$. Thus the on-rate constant is lower and the off-rate constant higher than that of amiloride (Table). The microscopic inhibition constant of $K_{5H}^{mi} = 4.02 \pm 2.64$ μM is significantly smaller than the macroscopic inhibition constant.

Competition of Two Organic Blockers

To study competition between amiloride and its 5H-analog we used the latter at a fixed concentration of 10 μM and added amiloride in

concentrations between zero and 7.2 μM (Fig. 4*B*). In spite of the presence of two species of blocking molecules, only one blocker-induced Lorentzian was clearly discernable in the frequency band 0.1 to 110 Hz. To find a theoretical basis for this observation we calculated double-Lorentzian spectra using competition kinetics and the rate constants of amiloride and 5H-amiloride. The calculations were conveniently done with the matrix method of Chen (1975). The result (Fig. 4*C*) shows that the difference between the two expected plateaus is at this combination of rate constants small and will hardly be resolved.

On increasing A_o in the presence of 10 μM 5H-amiloride, the plateau power decreased and the corner frequency increased. The corner frequencies were at all A_o clearly larger than those observed with amiloride alone, as shown in the rate-concentration plot of Fig. 4*D*. The data of the upper plot (amiloride plus analog) indicate a high valued ordinate intercept and a slightly smaller slope than the rate-concentration plot of amiloride in the absence of its analog (dashed line). Using unsimplified competition kinetics and the measured rate constants of amiloride and 5H-amiloride obtained from the same skin with only one of the organic blockers present, we calculated the chemical rate as a function of amiloride concentration for the presence of 10 μM 5H-amiloride (Fig. 4*D*, solid lines labeled λ_h). Good agreement with the measured values (open circles) was found.

The plateaus of the expected double Lorentzian should separate better if the analog competing with amiloride had a higher chemical rate than 5H-amiloride. For instance, the 6H-analog, which has an off-rate constant 30-fold larger than that of amiloride, should allow the plateaus to separate very well. This, too, was confirmed by spectra computed from competition kinetics. Power density spectra obtained in the presence of amiloride and 6H-amiloride showed the expected double-Lorentzians with separated plateaus (Fig. 5).

Triamterene

This is a Na-channel blocking diuretic like amiloride, but of rather different structure (6-phenyl-2,4,7 triaminopteridine) and less potent (Cuthbert & Shum, 1974). Hoshiko and Van Driessche (1981) used this compound to induce Na transport noise in frog skin epithelium. Christensen and Bindslev (1982) also used it as

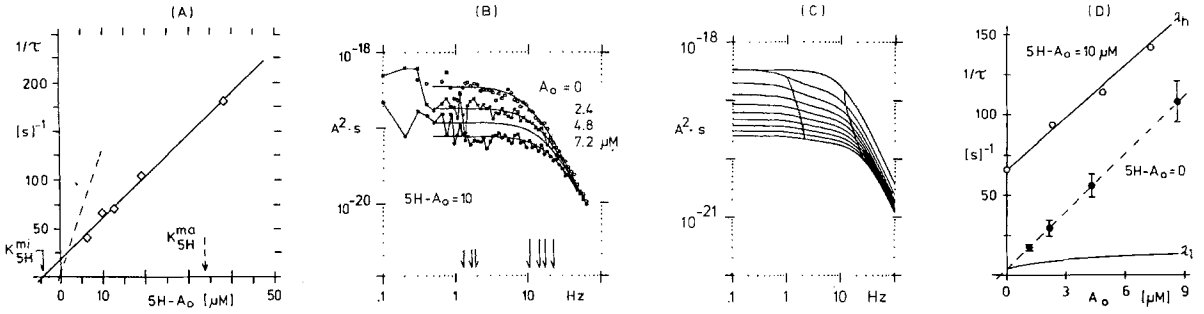

Fig. 4. Competition between amiloride and 5H-amiloride, analog L590,481-01H06. K-depolarized short-circuited frog skin, 3 cm^2, Na_o = 60 mM, mucosal pH 5.5. *A*: Rate-concentration plot of 5H-amiloride obtained in the absence of amiloride. For reference, the dashed line shows amiloride data from Fig. 2*B*. Note that the two lines cross. *B*: Current power density spectra obtained in the presence of 5H-amiloride (10 μM throughout) together with amiloride at the concentrations indicated. The data points for A_o = 4.8 μM were omitted for clarity. According to panel *A*, 5H-A is at low A_o the blocker of higher, but at high A_o the blocker of lower chemical rate. In the presence of two organic blockers double Lorentzian spectra were expected, but in the data only the higher frequency parts of the double Lorentzians are clearly discernable. The plateau decreases and the corner frequency increases (right group of arrows) when the amiloride concentration is raised. The left group of arrows marks the corner frequencies expected for the low frequency Lorentzians. For their calculation *see* panel *D*. *C*: Theoretical power-density spectra for two competing blockers. The set of curves simulates the data of panel *B*. Ordinate scale arbitrary. Parameters used: 5H-A_o = 10 μM throughout, with the rate constants k_{10} = 17.83 sec^{-1}, k_{01} = 4.82 sec^{-1} μM^{-1}; A_o = 0 to 9 μM in steps of 1 μM, with the rate constants k_{20} = 3.6 sec^{-1}, k_{02} = 12 · sec^{-1} μM^{-1}. The curved vertical lines indicate the corner frequencies of the component Lorentzians. The calculations show that the double Lorentzians expected for panel *B* will have well separated corner frequencies but poorly separated plateaus. *D*: Rate-amiloride concentration plot. The theoretical (solid) lines represent λ_h and λ_l, calculated for the presence of two extrinsic blockers from competition kinetics (Eq. 8b and 12 of Lindemann & Van Driessche, 1977). λ_h fits the data well. The apparent on- and off-rate constants of amiloride and of the 5H-analog, which are needed for this calculation, were determined separately for this skin. The dashed line (from Fig. 2*B*) is valid for amiloride in the absence of 5H-amiloride

an extrinsic blocker in their study of intestinal Na channels. Taking advantage of the reduced potency, we have used triamterene to study the natriferic response of apical Na channels to hormonal stimulation in the urinary bladder of *B. marinus* (*unpublished*). In the bladder, triamterene had a 10-fold higher off-rate constant than amiloride (*see* Table). As a consequence its Lorentzian spectra could be obtained at lower levels of blockage than are required when using amiloride. To compare the blocking kinetics of triamterene with those of amiloride in more detail, further experiments were done with the skin of *R. ridibunda*, for which a large number of data for amiloride and its structural analog have already been accumulated. Even higher off-rate constants of triamterene were found in this tissue.

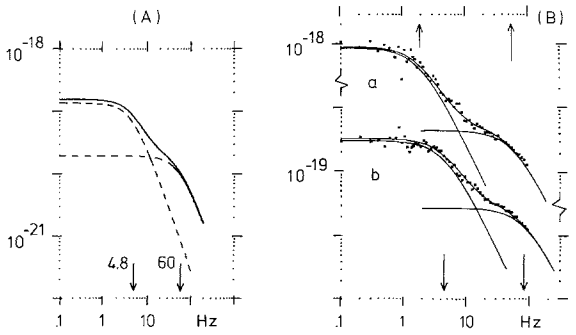

Fig. 5. *A*: Theoretical current power density spectra for competition of amiloride with 6H-amiloride. Parameters used: $A_o = 3.6\ \mu M$, $k_{20} = 5.32\ sec^{-1}$, $k_{02} = 14.8\ sec^{-1}\ \mu M^{-1}$; 6H-$A_o$ $= 12.23\ \mu M$, $k_{10} = 162.11\ sec^{-1}$, $k_{01} = 13.8\ sec^{-1}\ \mu M^{-1}$. The calculation shows that because of the high off-rate of the 6H-analog the plateaus of the double Lorentzian should separate very well. *B*: Power-density spectra [$A^2 \cdot sec$] recorded in the presence of amiloride and 6H-amiloride. Nondepolarized short-circuited frog skin of 3 cm^2 area, $Na_o = 60$ mM, mucosal pH 5.5, 6H-$A_o = 12.23\ \mu M$ for both spectra; $A_o = 1.8\ \mu M$ for spectrum (*a*) and 3.6 μM for spectrum (*b*). The Lorentzian components found by fitting are drawn in and their corner frequencies marked by arrows. In accordance with theoretical expectations (panel *A*), the plateaus separate well in both cases

Since triamterene (T) is a weaker base than amiloride, with a pK_a of 6.2 rather than 8.7 (Cuthbert, 1976), most triamterene experiments were performed at pH 5.5 in order to increase the concentration of the charged species (to about 83% of the total triamterene concentration, *see below*). Macroscopic dose-response curves, obtained in the presence of 60 mM Na_o from 12 preparations, yielded a mean K_T^{ma} of 18 μM. The data show considerable variation (Table). One example, where a K_T^{ma} of only 8.8 μM was found, is given in Fig. 6*A*. Note that due to the high off-rate constant the triamterene concentrations useful for noise analysis are on the low inhibition branch of the dose-response curve.

Sodium current fluctuations, observed in the presence of 1 to 10 μM triamterene, contained blocker-induced spectral components of Lorentzian shape (Fig. 6*B*). The plateau-power versus concentration plot is convex like that of 5,6-diCl-amiloride and the rate-concentration plot is linear (Fig. 6*C*), yielding the apparent rate constants listed in the Table. At pH 5.5 k_{on} is comparable to that of amiloride (dashed line),

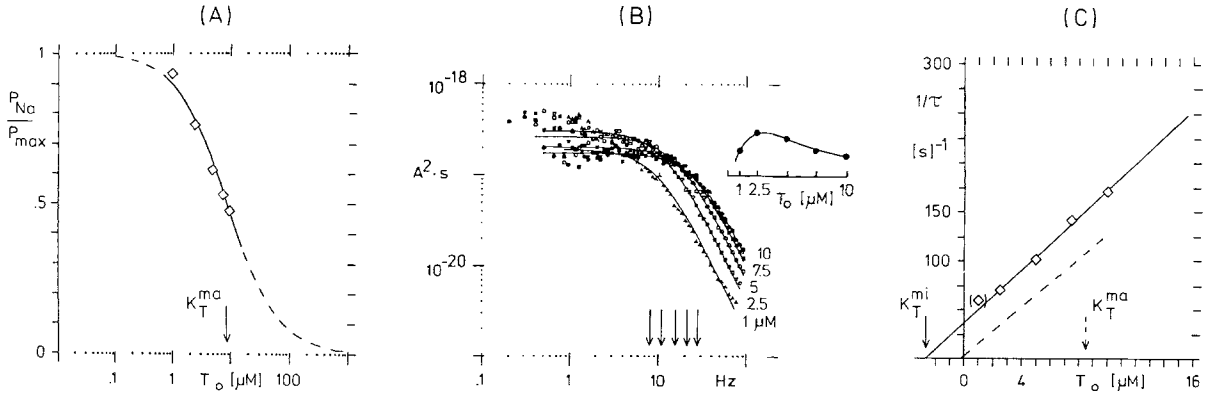

Fig. 6. Macroscopic and microscopic data obtained for 3 cm^2 of K-depolarized short-circuited frog skin in the presence of triamterene (T) and 60 mM Na_o, pH 5.5. *A*: Normalized macroscopic dose-response curve of one experiment. $K_T^{ma} = 8.8\ \mu M$. When the data point at 1 μM triamterene is excluded from the fit, K_T^{ma} changes insignificantly. *B*: Current power density spectra at $T_o = 1$, 2.5, 5, 7.5 and 10 μM. Preparation of panel *A*. Note that – in contrast to the amiloride spectra (Fig. 2*A*) – the maximum of the S_o versus concentration curve is covered by the data (inset). *C*: Rate-concentration plot $1/\tau_2 = 2\pi f_c^T \approx k_{on} T_o + k_{off}$ is plotted versus T_o. Preparation of panel *A* and *B*. The first data point was not included in the fitting of the regression line. Pooled data of 6 experiments gave a straight line relationship (*see* Fig. 7*B*). Note that again $K_T^{mi} = k_{off}/k_{on} < K_T^{ma}$. The dashed line is the amiloride rate-concentration relationship (Fig. 2*B*) given for comparison

while the off-rate constant is nearly 10 times larger than k_{off} of amiloride. From Fig. 6*C* K_T^{mi} was estimated to 2.7 μM. While the values of K_T^{ma} show considerable scatter (Table), each of them is larger than the K_T^{mi} obtained from the same epithelial preparation.

Experiments where amiloride and triamterene were used simultaneously showed that these two blockers also compete. The Na-channel currents (*i*) calculated from triamterene-induced Lorentzians were typically smaller (mean value 0.07 ± 0.01 pA; $n=14$) than those obtained with amiloride (0.10 ± 0.02 pA; $n=42$). The barely significant difference is understandable when considering that the triamterene concentrations used cause less inhibition of the macroscopic Na current than the amiloride concentrations used. The cellular Na activity may then be larger, decreasing the driving force for *i*. In addition *i* may in this case be somewhat underestimated, because the resistance of the K-depolarized basolateral membrane can be expected to increase with the cellular Na activity (*see* Fuchs et al., 1977).

pH-Dependence of the Apparent On-rate

From macroscopic dose-response curves Benos, Simon, Mandel and Cala (1976) concluded that the positively charged form of amiloride is the active blocker. The same conclusion was reached by Cuthbert (1976) with respect to several Na-channel blockers, including triamterene. Based on these results one would expect that a decrease in pH will have the same effect on the Lorentzian blocking spectra as an increase in the total chemical concentration of the blocker, i.e. a downward shift of the plateau power and an increase in corner frequency. As shown in Fig. 7*A* this expectation was confirmed for triamterene. The rate-concentration plot changed when the pH was lowered (Fig. 7*B*) such that the apparent on-rate constant (slope) increased while the off-rate constant remained unaffected (Table). The latter observation agrees with our previous conclusion (Li & Lindemann, 1981*b*) that the receptor properties are not pH-dependent in the pH range 7 to 5.5. Comparing k_{on} values obtained from the same preparation at pH 7 and 5.5, we found a ratio of 0.37 ± 0.07 ($n=8$). This value is about 20% smaller than expected from the reported first pK_a of triamterene (6.2, *see* Cuthbert, 1976). A better agreement can hardly be expected since triamterene has more than one ionizable group, the doubly charged compound possibly being ineffective as a blocker. In addition, the concentration of the monovalent free base may have been lowered further by complex-formation (*see* Dittert, Higuchi & Reese, 1964).

In conclusion, compared to amiloride, a lower basicity and a shorter blocking time based mainly on a higher off-rate constant account for the poorer blocking efficacy of triamterene.

Triaminopyrimidine (TAP)

While this molecule was first used as a blocker of the paracellular pathway of leaky epithelia

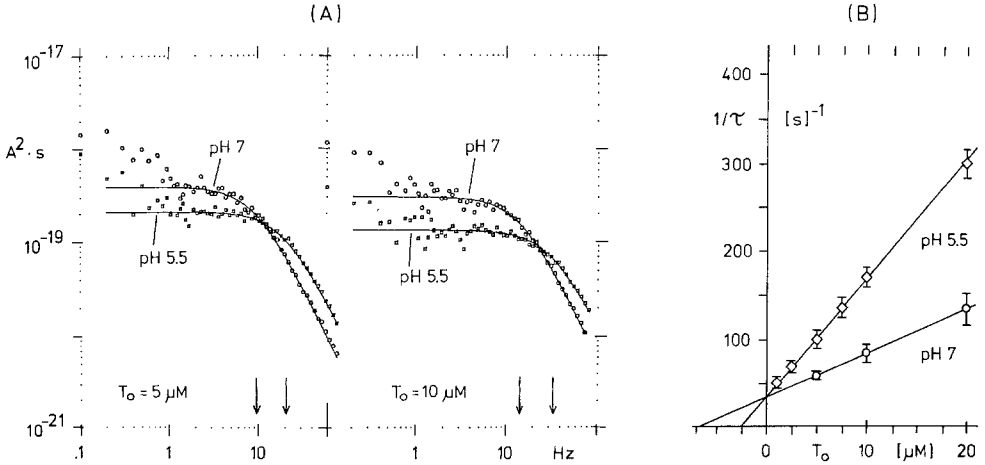

Fig. 7. The pH dependence of the channel blocking kinetics of triamterene (T) in K-depolarized short-circuited frog skin, 3 cm^2, $Na_o = 60$ mM. *A*: Current power density spectra at $T_o = 5$ (left panel) and at $T_o = 10$ μM (right panel) for an apical pH 7.0 (upper) or pH 5.5 (lower spectra). At the same triamterene concentration the corner frequency of the Lorentzian is higher and the plateau lower at pH 5.5 compared to pH 7.0. Thus, at low pH more blocker molecules seem to be present. *B*: Upper characteristic rate versus total triamterene concentration at two apical pH values. Mean values (±SD) are shown. The number of measurements *n* at pH 7.0 was 6; that at pH 5.5 was also 6 for $T_o = 5$, 7.5 and 10 μM, but for $T_o = 1$ and 2.5 μM, $n=5$ and for $T_o = 20$ μM, $n=3$. The increased on-rate (slope) at lower pH indicates that the positively charged molecule is the blocking species

(Moreno, 1974), it is also a reversible blocker of apical Na channels (Zeiske, 1975). Using macroscopic methods, Balaban, Mandel and Benos (1979) established that TAP and amiloride are competitive blockers. The first pK_a value is 6.72 (Roth & Strelitz, 1969). At pH 5.5, therefore, about 94% of the TAP molecules should be charged. At this pH a mean K_{TAP}^{ma} of 4.15 mM was obtained in the presence of 60 mM Na_o from 11 macroscopic dose-response curves. The current fluctuations observed with 60 mM Na_o showed in the presence of 1 mM TAP a uniform depression of power densities between 0.1 and 110 Hz, but no blocker-induced Lorentzian components (Fig. 8*A*). It may be suspected that the off-rate of TAP is high, such that the chemical rate of channel blocking considerably exceeds 110 Hz. Provided TAP would compete with amiloride, we should then see systematic changes in amiloride-induced Lorentzian plateaus and corner frequencies. This turned out to be the case. Figure 8*B* shows that the induced Lorentzian observed with 9.6 μM amiloride attains a smaller corner frequency when 100 μM TAP is added to the solution. This depression of corner frequency is expected for the Lorentzian of an extrinsic blocker when a competitive blocker of higher chemical rate is added (*see* Lindemann & Van Driessche, 1978). As a consequence, the linear rate-concentration plot of amiloride (Fig. 8*C*) shows in the presence of TAP a clear decrease in slope (apparent on-rate). For the case of a very fast blocker like TAP being present together with amiloride, it can be shown that the slopes of the amiloride rate concentration plot obtained in the absence and presence of the faster blocker obey the relationship

$$\frac{\text{slope } (TAP_o = 0)}{\text{slope } (TAP_o > 0)} = 1 + \frac{TAP_o}{K_{TAP}}. \qquad (16)$$

From four experiments a value of $K_{TAP} \approx K_{TAP}^{mi} = 0.33 \pm 0.08$ mM was thus calculated. Note that again the microscopic inhibition constant turns out to be smaller than the macroscopic inhibition constant. The ratio of these constants remains the same after correction for incomplete protonation. The correction lowers K_{TAP}^{mi} to 0.31 mM and K_{TAP}^{ma} to 3.90 mM.

Alternatively, the microscopic inhibition constant of TAP can be calculated based on the change of K_A^{ma} of amiloride estimated from macroscopic dose-response data obtained in the presence and absence of TAP. However, due to the self-inhibition effect this change is less sensitive to the presence of TAP than the change in the apparent slope of the rate-concentration plot. As shown in Fig. 8*D*, at $TAP_o = 0.1$ mM there was no noticeable change in the K_A^{ma} of amiloride (open squares), but when the TAP concentration had been increased to 1 mM the K_A^{ma} increased from 1.27 to 1.88 μM (filled squares). Using the $K_A^{mi} = 0.12$ μM of amiloride, derived from the rate-concentration plot data of the same skin, we calculate a value of 0.20 mM for the K_{TAP}^{mi}, which is to be compared with the value of 0.33 mM obtained from noise data.

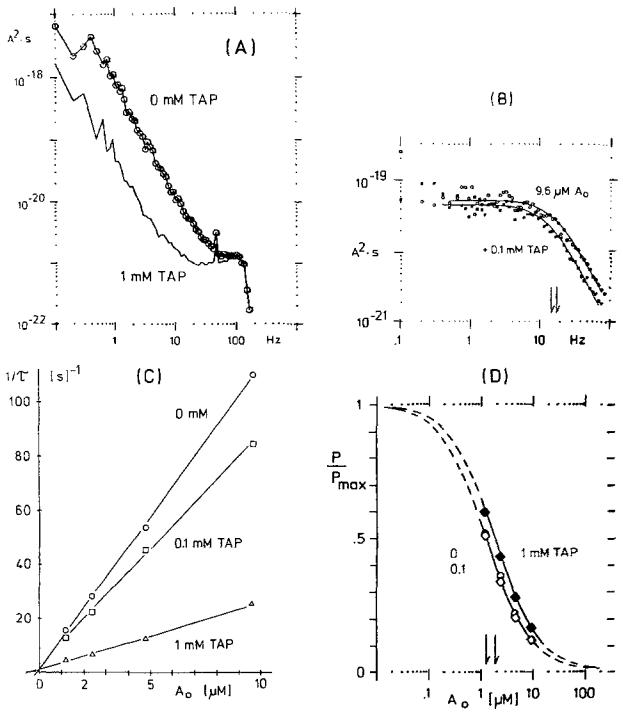

Fig. 8. Competition between amiloride and triaminopyrimidine (TAP). K-depolarized short-circuited frog skin. 3 cm^2 area, $Na_o = 60$ mM, mucosal pH 5.5. *A*: Current power density spectra in the absence and presence of TAP. At TAP = 0.1 mM, the spectrum is nearly identical to the one taken in the absence of TAP. At TAP = 1 mM, the power is reduced but no clear Lorentzian components are visible in the frequency range used. *B*: Current power density spectra in the presence of 9.6 μM amiloride alone (upper) and together with 0.1 mM TAP (lower curve). At this low concentration of TAP no significant inhibition of the macroscopic Na current occurred, but a decrease of the corner frequency (arrows) of the amiloride-induced Lorentzian is already discernible. *C*: Rate-amiloride concentration plot. Note that the apparent on-rate (slope) becomes smaller as the concentration of the higher rate competitor, TAP, is increased. Evaluation of the slope ratio with Eq. (16) yields $K_{TAP}^{mi} = 0.32$ and 0.29 mM, respectively. *D*: Normalized dose-response curve of amiloride in the absence (◇) and presence of 0.1 mM (○) and 1 mM (◆) TAP. The change in K_A^{ma} is seen to be much less sensitive to the presence of TAP than the change in slope of the rate-concentration plot (panel *C*). At 0 and 0.1 mM of TAP, the K_A^{ma} was practically identical, being 1.27 μM. At 1 mM TAP, the K_A^{ma} was 1.88 μM

Discussion

Rate Constants

Of the 5 organic cations, 4 could be analyzed with respect to blocking rate constants. We found for 5,6-diCl-amiloride, 5H-amiloride and triamterene, just as for amiloride, the higher chemical rate of block to be a linear function of blocker concentration (pseudo-first-order). The off-rate constants range between 4 and 150 sec^{-1}, the mean time of channel blockage, therefore, between 6 and 250 msec.

The off-rate constants of amiloride and triamterene do not show a significant pH dependence (between pH 5.5 and 7.5), but the (apparent) on-rate constants do, provided the blocker has a low pK_a as in the case of triamterene (Table). Here the on-rate increases when the pH is lowered from 7 to 5.5, indicating that the positively charged drug species is the active blocker, as proposed by others (Benos et al., 1976; Cuthbert, 1976). This conclusion is strengthened by the observation that blockers of high pK_a, like amiloride, show only a weak pH-dependence of k_{on} (Li & Lindemann, 1981*b*). Since the off-rates were found insensitive to pH, it appears that the structure at the Na channel which controls binding and release of the blocking molecule does not change properties significantly between pH 5.5 and 7. (However, at pH 5.5 more Na channels are made available for transport (Li & Lindemann, 1981*b*).)

The data show, furthermore, that the apparent on-rate constant of the protonated blocker is smaller than expected for a diffusion-limited approach to the blocking site, and depends strongly on the structure of the blocker. However, since the rate concentration plots are linear, k_{on} does not depend on the concentration of the blocker. The lowest k_{on} was found with 5H-amiloride in frog skin (3.4 $sec^{-1}\,\mu M^{-1}$), the highest with triamterene in toad bladder (64 $sec^{-1}\,\mu M^{-1}$; *see* Table). The structure dependence of the on-rate constant could result from steric hindrance or from a brief interaction of blocking molecule and channel, which would have to occur before a blocking position of longer lifetime is attained. This point will be discussed in detail in a following paper (Li, Cragoe & Lindemann, *in preparation*).

Competition Between Two Extrinsic Blockers

Model calculations based on unsimplified kinetics of three competing reactions have shown that in the presence of two organic blockers the corner frequencies of their spectra may be increased by self-inhibition. However, provided their blocking rates are comparable to those of amiloride, the effect will be no larger than with amiloride, where it may be considered small (*see below*). Therefore spectra of two competing high rate blockers were in first approximation analyzed neglecting the self-inhibition.

The case of amiloride plus 5H-amiloride was studied in more detail. Keeping the concentration of 5H-amiloride constant and varying that of amiloride, we expected power density spectra of double-Lorentzian shape. However, in the recorded spectra (Fig. 4*B*) only the Lorentzian component predicted at higher frequencies could be clearly distinguished. Nevertheless, its change with amiloride concentration conformed well to competition theory (Fig. 4*D*). It may be suspected that with the given set of rate constants the Lorentzian component of lower corner frequency cannot rise clearly above the plateau of the higher frequency component. To check this point we calculated double-Lorentzian spectra for competition of two blockers, using the rate constants of amiloride and 5H-amiloride obtained experimentally. The result (Fig. 4*C*) verifies that the two plateaus will not separate very well, since the corner frequencies differ by less than one decade. However, if the chemical rates of the two blockers are further apart, as in the case of amiloride and 6H-amiloride, a good separation of the plateaus is found (Fig. 5).

In conclusion, then, the expected effects of competition were found in the recorded spectra. A more detailed analysis will require more analog material than was available to us in the course of this study.

Competition Between Na Self-Inhibition and Organic Blockers In Macroscopic Studies

Evidence for competition between Na_o and amiloride in their blocking effects on Na transport has been accrued from steady-state dose-response curves in a variety of studies. The question usually discussed is, whether the competition is kinetically pure, or to which extent it is mixed. Pure competition has already been formalized (*see* Theory, Eq. 5). In mixed inhibition the reaction scheme includes the additional state N_{12} in which the channel is simultaneously closed by the self-inhibition and blocked by amiloride

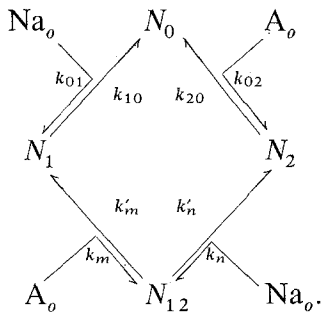

The transitions $N_1 \rightleftharpoons N_{12}$ and $N_2 \rightleftharpoons N_{12}$ are electrically silent. There are two additional dissociation constants

$$K'_A = \frac{k'_m}{k_m} \quad \text{and} \quad K'_N = \frac{k'_n}{k_n}$$

of which one needs to be known. The other is then obtained from the principle of microscopic reversibility. The macroscopic inhibition constant is given by

$$K_A^{ma} = K_A \cdot \frac{1 + \frac{Na_o}{K_N}}{1 + \frac{Na_o}{K_N} \cdot \frac{K_A}{K'_A}}. \tag{5a}$$

$K_A = K'_A$ means pure noncompetitive inhibition, where K_A^{ma} equals K_A at all Na$_o$. With $K'_A \gg K_A$ pure competitive inhibition results, where K_A^{ma} is a linear function of Na$_o$. For intermediate values of K'_A mixed inhibition will ensue, with K_A^{ma} being a saturating function of Na$_o$. In the latter case, the larger the degree of competitive behavior, the more will K_A^{ma} exceed K_A.

The early demonstration by Cuthbert and Shum (1974) of seemingly pure competitive behavior in skins of *R. temporaria* was confirmed for *R. esculenta* (*ridibunda*) (Zeiske & Lindemann, 1974; *see also* Lindemann, 1977, Fig. 6, and Cuthbert, 1981). It was also confirmed for toad urinary bladder (Sudou & Hoshi, 1977). Aceves and Cuthbert (1979) found pure competition between Na and the amiloride analog benzamil in skins of *R. temporaria*. While Benos, Mandel and Balaban (1979) described noncompetitive inhibition for the skins of *R. catesbeiana* and *R. pipiens*, they found mixed inhibition for the skin of *R. temporaria*. In contrast, Takada and Hayashi (1980) observed mixed inhibition with the skin of *R. catesbeiana*. Mixed inhibition was also described for the rabbit descending colon (Turnheim, Luger & Grasl, 1981). In the hen coprodaeum weak competitive inhibition was found (Bindslev, Cuthbert, Edwardson & Skadhauge, 1982). Microsomes derived from toad urinary bladder also show competition (Labelle & Valentine, 1980). Finally, amiloride is also competitive with Na in its blocking effect on the Na/H exchange (Vigne, Frelin & Lazdunski, 1982). In short, the type of interaction between blockage by Na and amiloride appears variable among species and tissues, but for skins of *R. temporaria* and *R. esculenta* (*ridibunda*) only pure competition or, in one instance, mixed inhibition has been found.

All these steady-state studies do not clearly distinguish between inhibition by Na ions from the mucosal side of the membrane (self-inhibition) and from the cellular side (feedback inhibition, e.g. Taylor & Windhager, 1979). The existence of the self-inhibition as such was deduced from the timecourse of I_{Na} following a rapid increase of Na$_o$. While the inhibition developed, Na$_c$ remained small and nearly constant (Fuchs et al., 1977). The observed inhibition time constants in the order of seconds imply that the corner frequency of a 'Na-induced Lorentzian' representing the self-inhibition will be difficult to demonstrate by steady-state noise analysis, as discussed below.

Evidence for Competition from Noise Analysis

A clear demonstration of Na-induced Lorentzians in current power density spectra has so far failed, in part because of superposition of drift effects. Other interfering effects have been discussed (Lindemann & Van Driessche, 1978; Lindemann, 1980). However, in voltage power density spectra of frog skin a Na-induced Lorentzian of low corner frequency was found (Van Driessche & Borghgraef, 1975).

By analysis of amiloride-induced Lorentzians it was found that N_0 decreases when Na$_o$ is increased (Van Driessche & Lindemann, 1978). While this result is expected from self-inhibition, it is also explicable by Na dependent noncompetitive inhibition, as in the case of the hen coprodaeum (Christensen & Bindslev, 1982). However, in toad urinary bladder the sum $N_0 + N_2$ (Eq. 14) increased with A$_o$ (Li et al., 1982), just as in skins of *R. esculenta* (Li & Lindemann, 1983). This indicates competition with Na$_o$ or, perhaps, release from an Na$_c$-dependent block. However, with the high A$_o$ used, Na$_c$ must have been small and, therefore, feedback effects from Na$_c$ minimal.

In frog skin PCMPS and BIG, agents which abolish the Na self-inhibition to a large extent

(Zeiske & Lindemann, 1974; Dick & Lindemann, 1975) were found to diminish the increase of N_0+N_2 with A_o (Li & Lindemann, 1983). For the presence of BIG or PCMPS one would expect that k_{off} is lowered towards k_{20} (Eq. 8). With PCMPS this was actually observed. With 60 mM Na_o k_{off} decreased from 3.13 ± 0.33 to 2.09 ± 0.27 sec^{-1} (Li & Lindemann, 1983). This result indicates that $k_{off}>k_{20}$ and $K_A^{mi}\approx K_A\cdot 1.5$, due to the self-inhibition effect. Using Eq. (8) we find that k_{01} must be in the order of 0.017 sec^{-1} mM^{-1}. This is a small value, but numerically significant because k_{20} is also small. With BIG a decrease of K_A^{mi} was not observed.

Van Driessche and Lindemann (1979) obtained the apparent rate constants of amiloride at different Na_o in K-depolarized skins of *R. esculenta*. They found k_{on} to be independent of Na_o while k_{off} seemed to increase when Na_o was raised from 6 to 60 mM. However, in terms of corner frequencies this effect was very small, only 1 Hz or a 10% increase. It can be debated whether this was a significant change. Hoshiko and Van Driessche (1981) recently found that k_{off} of triamterene, which is larger and therefore more easily measured, did not significantly change with Na_o.

A small k_{01} is of course difficult to estimate from corner frequencies and may be more easily obtained from macroscopic experiments. Using fast concentration jumps, Lindemann and Gebhardt (1973) estimated the time constant of the Na self-inhibition with increasing steps of Na_o for skins of *R. esculenta*. A value of 3.6 sec was found for a concentration step from 0 to 74 mM activity. This implies the very low corner frequency of $f_c^N=0.044$ Hz for the self-inhibition. From

$$1/\tau_1=2\pi f_c^N=k_{10}\cdot(1+Na_o/K_N) \tag{7a}$$

the rate constants may be calculated. For $K_N=10$ mM and $Na_o=60$ mM we obtain $k_{10}=0.033$ sec^{-1} and $k_{01}=0.0033$ sec^{-1} mM^{-1}. This value of k_{01} implies that $k_{01}\cdot Na_o$ makes a nearly insignificant contribution to k_{off} of τ_{-2}.

In short, the analysis of Lorentzian plateaus indicates a competitive component in the blocking of channels at 60 mM Na_o. The analysis of blocking rate constants indicates tentatively that k_{off} may exceed k_{20} by a factor between 1 and 2. Of course, even if better data will in the future show that k_{off} equals k_{20}, this is entirely compatible with a competition mechanism, and, in fact, expected from the high value of τ_1 observed with concentration jumps.

The Relationship of K^{ma} and K^{mi}

By combining Eq. (6a) with Eq. (5a) we obtain

$$\frac{K^{ma}}{K^{mi}}=\frac{(1+Na_o/K_N)}{\frac{k_{off}}{k_{20}}\left(1+\frac{Na_o}{K_N}\cdot\frac{K_A}{K'_A}\right)}. \tag{17}$$

The relationship shows that in the case of pure competition K^{ma} will be significantly larger than K^{mi}, provided k_{off} does not exceed k_{20} too much. For $Na_o=60$ mM, $K_N=10$ mM and $k_{off}=k_{20}$, K^{ma} will exceed K^{mi} by a factor of 7. In the case of mixed inhibition and the same K_N the factor will be smaller and for noncompetitive inhibition the ratio will be unity. In this case k_{off} will be identical with k_{20}.

Experimentally we found for all blockers investigated K^{ma}/K^{mi} significantly larger than unity. The smallest ratio of about 2 was found for amiloride and triamterene in toad bladder, the largest ($\approx$12) for TAP in frog skin. Excluding TAP, for which K^{mi} was estimated rather indirectly, we find with frog skin and 60 mM Na_o that the values of this ratio are, for the remaining four molecules, reasonably close together, ranging between 6 and 8.3 (Table).

In Fig. 9*A*, the K^{ma} values found for the five blockers are plotted against the corresponding K^{mi} values in double-logarithmic coordinates. The dashed line is the expected relationship $K^{ma}=K^{mi}$ for noncompetitive inhibition. The drawn-out line corresponds to $K^{ma}=7.0\cdot K^{mi}$. It can be seen that within the experimental error a proportionality constant of 7.0 fits the data reasonably well, particularly when the TAP data, where K^{mi} is least reliable, are excluded.

According to Eq. (17) this result is compatible with pure competitive or with mixed inhibition. For $k_{off}=k_{20}$ and pure competition a K_N value of 10 mM would be implied. It is well within the range of apparent K_N values found previously (5 to 25 mM, *see* Fuchs et al., 1977, Fig. 11). In the case of mixed inhibition the real K_N value would be smaller than 10 mM.

Should mixed inhibition be present, it would be interesting to estimate the proportion of competitive and noncompetitive behavior as expressed by the relative values of K_A and K'_A. Rearrangement of Eq. (17) yields

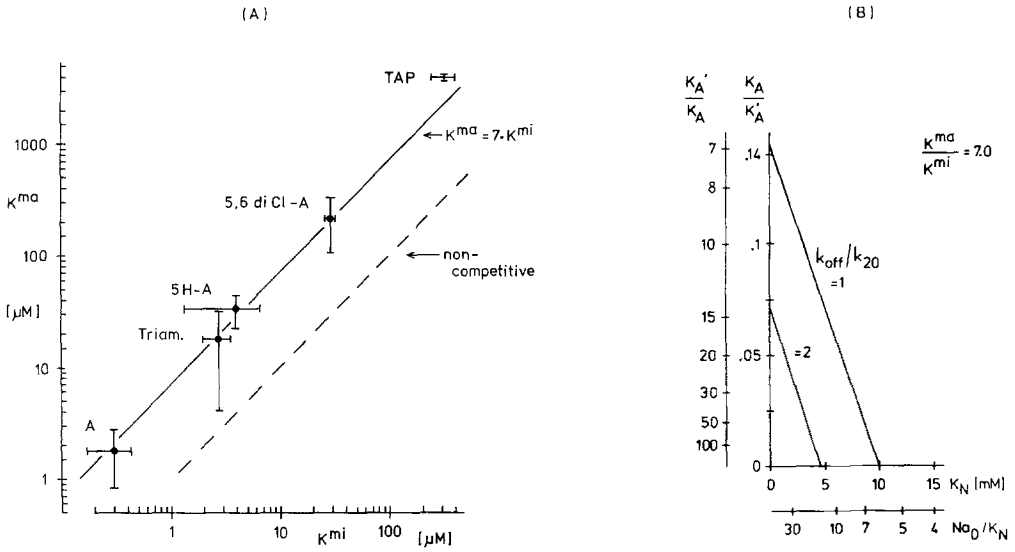

Fig. 9. *A*: Relationship of K^{ma} and K^{mi} for the five organic blockers used at pH 5.5 and 60 mM Na_o. Frog skin data of the Table; the values were not corrected for pK_a. The bars denote standard deviations. The dashed line is the expected relationship for $K^{ma} = K^{mi}$, i.e. for noncompetitive inhibition. The solid line was drawn for $K^{ma}/K^{mi} = 7.0$ (pure competitive or mixed inhibition, Eq. 17). *B*: Theoretical dependence (Eq. 17a) of the relative values of K_A and K_A' on K_N, drawn for $K^{ma}/K^{mi} = 7.0$ (*see* panel *A*). For typical values of $K_N > 5$ mM, the diagram indicates $K_A' \gg K_A$, i.e. that the noncompetitive component is negligible

$$\frac{K_A}{K_A'} = \frac{\left(1 + \frac{Na_o}{K_N}\right) - \frac{K^{ma}}{K^{mi}} \cdot \frac{k_{off}}{k_{20}}}{\frac{Na_o}{K_N} \cdot \frac{K^{ma}}{K^{mi}} \cdot \frac{k_{off}}{k_{20}}}. \qquad (17a)$$

In Fig. 9*B* the theoretical dependence of K_A/K_A' on K_N is plotted for $K^{ma}/K^{mi} = 7.0$. The parameter k_{off}/k_{20} was set to 1.0 or 2.0. It can be seen that K_N values $\leqq 10$ mM and ratios $K_A'/K_A \geqq 7.0$ are compatible with the observed K^{ma}/K^{mi}. Therefore, although the competition may be mixed, the competitive behavior must be dominating. For the expected K_N values, which range above 5 mM (*see* Fuchs et al., 1977), Fig. 9*B* suggests that the noncompetitive component is negligible in the skin of *R. esculenta*. Interestingly, in the hen coprodaeum, where the competitive component is not as dominant (Bindslev et al., 1982), K_T^{ma} barely exceeds K_T^{mi} (Christensen & Bindslev, 1982).

In summary, then, the low chemical rate of the self-inhibition effect precludes a clear demonstration of its competition with extrinsic blockage by amiloride, by means of rate analysis alone. However, the competition becomes apparent in the plateau analysis and by combination of rate analysis with macroscopic techniques. Pure competition or the competitive component of mixed inhibition will be evident from K^{ma} increasing with Na_o and being larger than K^{mi} (Fig. 9). In the system investigated, competitive behavior exceeds noncompetitive behavior by a factor of 7 or more.

Which Extrinsic Blocker is Suited Best?

Given a set of extrinsic blockers of different chemical rates, which one will be most suitable to be used in the analysis of single-channel currents and the area density of channels? With single membrane preparations it is sufficient to select a blocker of a chemical rate which matches the frequency band to be used. In addition, the off-rate should not be too small to be estimated with accuracy. In cases where competition prevails, a large difference of the chemical rates of the competitors will simplify the analysis. In those cases where the noise current passes two membranes it is advisable to select a blocker which meets the above requirements and, in addition, yields analyzable Lorentzians at a high level of fractional inhibition. Thereby, the cellular Na-activity will be kept low, and in consequence the single-channel current will not change very much with the blocker concentration. Furthermore, changes of channel density mediated by the cellular Na activity (feedback inhibition; *see* Grinstein &

Erlij, 1978; Taylor & Windhager, 1979; Chase & Al-Awqati, 1981) will then be minimal. Finally, if the basolateral membrane is K-depolarized, its resistance and, therefore, its filter effect (Van Driessche & Goegelein, 1980; Lindemann & DeFelice, 1981) will remain tolerably small for all blocker concentrations used.

Our thanks are due to Frau Birgit Hasper and Herrn Gert Ganster for technical assistance and servicing of the electronics. Dr. T.D. Plant kindly improved the English of this paper. Amiloride-HCl-dihydrate was a gift from Sharp & Dohme GmbH, München. Germany, and its analogs were gifts from Dr. E.J. Cragoe, Jr., of Merck, Sharp, Dohme Research Laboratories, West Point, Pennsylvania, to whom our thanks are due. We also thank Röhm-Pharma GmbH, Darmstadt, Germany, for supplying triamterene.

This work was supported by the Deutsche Forschungsgemeinschaft through SFB 38, project C1.

References

Aceves, J., Cuthbert, A.W. 1979. Uptake of [^{3}H] benzamil at different sodium concentrations. Inferences regarding the regulation of sodium permeability. *J. Physiol. (London)* **295**:491–504

Balaban, R.S., Mandel, L.J., Benos, D.J. 1979. On the cross-reactivity of amiloride and 2,4,6 triaminopyrimidine (TAP) for the cellular entry and tight junctional cation permeation pathways in epithelia. *J. Membrane Biol.* **49**:363–390

Benos, D.J., Mandel, L.J., Balaban, R.S. 1979. On the mechanism of the amiloride-sodium entry site interaction in anuran skin epithelia. *J. Gen. Physiol.* **73**:307–326

Benos, D.J., Simon, S.H., Mandel, L.J., Cala, P.M. 1976. Effects of amiloride and some of its analogues on cation transport in isolated frog skin and thin lipid bilayers. *J. Gen. Physiol.* **68**:43–63

Bindslev, N., Cuthbert, A.W., Edwardson, J.M., Skadhauge, E. 1982. Kinetics of amiloride action in the hen coprodaeum *in vitro*. *Pfluegers Arch.* **392**:340–346

Chase, H.S., Jr., Al-Awqati, Q. 1981. Regulation of the sodium permeability of the luminal border of toad bladder by intracellular sodium and calcium. *J. Gen. Physiol.* **77**:693–712

Chen, Y.D. 1975. Matrix method for fluctuations and noise in kinetic systems. *Proc. Natl. Acad. Sci. USA* **72**:3807–3811

Christensen, O., Bindslev, N. 1982. Fluctuation analysis of short-circuit current in a warm-blooded sodium-retaining epithelium: Site current, density, and interaction with triamterene. *J. Membrane Biol.* **65**:19–30

Cuthbert, A.W. 1976. Importance of guanidinium groups for blocking sodium channels in epithelia. *Mol. Pharmacol.* **12**:945–957

Cuthbert, A.W. 1981. Sodium entry step in transporting epithelia: Results of ligand-binding studies. *In:* Ion Transport by Epithelia. S.G. Schultz, editor. pp. 181–195. Raven, New York

Cuthbert, A.W., Shum, W.K. 1974. Binding of amiloride to sodium channels in frog skin. *Mol. Pharmacol.* **10**:880–891

Dick, H.J., Lindemann, B. 1975. Saturation of Na-current into frog skin epithelium abolished by PCMPS. *Pfluegers Arch.* **355**:R72

Dittert, L.W., Higuchi, T., Reese, D.R. 1964. Phase solubility technique in studying the formation of complex salts of triamterene. *J. Pharm. Sci.* **53**:1325

Fuchs, W., Hviid Larsen, E., Lindemann, B. 1977. Current voltage curve of sodium channels and concentration dependence of sodium permeability in frog skin. *J. Physiol. (London)* **267**:137–166

Grinstein, S., Erlij, D. 1978. Intracellular calcium and the regulation of sodium transport in the frog skin. *Proc. R. Soc. London B* **202**:353–360

Hammes, G.G. 1968. Relaxation spectrometry of biological systems. *Adv. Protein Chem.* **23**:1–55

Hoshiko, T., Van Driessche, W. 1981. Triamterene-induced sodium current fluctuations in frog skin. *Arch. Int. Physiol. Biochim.* **89**:P58–P60

Labelle, E.F., Valentine, M.E. 1980. Inhibition by amiloride of $^{22}Na^+$ transport into toad bladder microsomes. *Biochim. Biophys. Acta* **601**:195–205

Li, J.H.-Y., Lindemann, B. 1981*a*. Blockage of epithelial Na-channels by organic cations: The relationship of microscopic and macroscopic inhibition constants. *Pfluegers Arch.* **391**:R25

Li, J.H.-Y., Lindemann, B. 1981*b*. pH dependence of apical Na transport in frog skin. *Adv. Physiol. Sci.* **3**:151–155

Li, J.H.-Y., Lindemann, B. 1983. Chemical stimulation of Na Transport through amiloride blockable channels of frog skin epithelium. *J. Membrane Biol. (in press)*

Li, J.H.-Y., Palmer, L.G., Edelman, I.S., Lindemann, B. 1982. The role of Na-channel density in the natriferic response of the toad urinary bladder to an antidiuretic hormone. *J. Membrane Biol.* **64**:77–89

Lindemann, B. 1977. A modifier-site model for passive Na transport into frog skin epithelium. *In:* Intestinal Permeation. M. Kramer and F. Lauterbach, editors. pp. 217–228. Excerpta Medica, Amsterdam

Lindemann, B. 1980. The beginning of fluctuation analysis of epithelial ion transport. *J. Membrane Biol.* **54**:1–11

Lindemann, B., DeFelice, L.J. 1981. On the use of general network functions in the evaluation of noise spectra obtained from epithelia. *In:* Ion Transport by Epithelia. S.G. Schultz, editor. pp. 1–13. Raven, New York

Lindemann, B., Gebhardt, U. 1973. Delayed changes of Na-permeability in response to steps of $(Na)_o$ at the outer surface of frog skin and toad bladder. *In:* Transport Mechanisms in Epithelia. H.H. Ussing and N.A. Thorn, editors. pp. 115–127. Munksgaard, Copenhagen

Lindemann, B., Van Driessche, W. 1977. Sodium specific membrane channels of frog skin are pores: Current fluctuations reveal high turnover. *Science* **195**:292–294

Lindemann, B., Van Driessche, W. 1978. The mechanism of Na uptake through Na-selective channels in the epithelium of frog skin. *In:* Membrane Transport Processes. J.F. Hoffman, editor. Vol. 1, pp. 155–178. Raven, New York

Moreno, J.H. 1974. Blockage of cation permeability across the tight junctions of gallbladder and other leaky epithelia. *Nature (London)* **251**:150–151

Palmer, L.G., Edelman, I.S., Lindemann, B. 1980. Current-voltage analysis of apical sodium transport in toad urinary bladder: Effects of inhibitors of transport and metabolism. *J. Membrane Biol.* **57**:59–71

Palmer, L.G., Li, J.H.-Y., Lindemann, B., Edelman, I.S. 1982. Aldosterone control of the density of Na-chan-

nels in the toad urinary bladder. *J. Membrane Biol.* **64**:91–102

Rick, R., Dörge, A., Nagel, W. 1975. Influx and efflux of sodium at the outer surface of frog skin. *J. Membrane Biol.* **22**:183–196

Roth, B., Strelitz, J.Z. 1969. The protonation of 2,4-diaminopyrimidines. I. Dissociation constants and substituent effects. *J. Org. Chem.* **34**:821

Sudou, K., Hoshi, T. 1977. Mode of action of amiloride in toad urinary bladder: An electrophysiological study of the drug action on sodium permeability of the mucosal border. *J. Membrane Biol.* **32**:115–132

Takada, M., Hayashi, H. 1980. Interaction of cadmium, calcium, and amiloride in the kinetics of active sodium transport through frog skin. *Jpn. J. Physiol.* **31**:285–303

Taylor, A., Windhager, E.E. 1979. Possible role of cytosolic calcium and Na-Ca exchange in regulation of transepithelial sodium transport. *Am. J. Physiol.* **236**:F505–F512

Turnheim, K., Luger, A., Grasl, M. 1981. Kinetic analysis of the amiloride-sodium entry site interaction in rabbit colon. *Mol. Pharmacol.* **20**:543–550

Van Driessche, W., Borghgraef, R. 1975. Noise generated during ion transport across frog skin. *Arch. Int. Physiol. Biochim.* **83**:140–142

Van Driessche, W., Goegelein, H. 1980. Attenuation of current and voltage noise signals recorded from epithelia. *J. Theor. Biol.* **86**:629–648

Van Driessche, W., Lindemann, B. 1978. Low-noise amplification of voltage and current fluctuations arising in epithelia. *Rev. Sci. Instrum.* **49**:52–55

Van Driessche, W., Lindemann, B. 1979. Concentration-dependence of currents through single sodium-selective pores in frog skin. *Nature (London)* **282**:519–520

Vigne, P., Frelin, C., Lazdunski, M. 1982. The amiloride-sensitive Na^+/H^+ exchange system in skeletal muscle cells in culture. *J. Biol. Chem.* **257**:9394–9400

Zeiske, W. 1975. The influence of 2,4,6-triamino-pyrimidine on Na-transport in frog skin. *Pfluegers Arch.* **359**:R127

Zeiske, W., Lindemann, B. 1974. Chemical stimulation of Na current through the outer surface of frog skin epithelium. *Biochim. Biophys. Acta* **352**:323–326

Received 28 March 1983; revised 13 May 1983